Automatica 75 (2017) 46–53

Contents lists available at ScienceDirect

Automatica

journal homepage: www.elsevier.com/locate/automatica

Brief paper

Angular velocity nonlinear observer from vector measurements ☆

Lionel Magnis, Nicolas Petit

MINES ParisTech, PSL Research University, CAS, 60 bd Saint-Michel, 75272 Paris Cedex, France

ARTICLE INFO

Article history:
Received 8 October 2014
Received in revised form
4 September 2015
Accepted 24 August 2016

Keywords:
Sensor and data fusion
Nonlinear observer and filter design
Time-varying systems
Guidance navigation and control

ABSTRACT

This paper proposes a technique to estimate the angular velocity of a rigid body from vector measurements. Compared to the approaches presented in the literature, it does not use attitude information nor rate gyros as inputs. Instead, vector measurements are directly filtered through a nonlinear observer estimating the angular velocity. Convergence is established using a detailed analysis of the linear-time varying dynamics appearing in the estimation error equation. This equation stems from the classic Euler equations and measurement equations. A high gain design allows to establish local uniform exponential convergence. Simulation results are provided to illustrate the method.

1. Introduction

This article considers the question of estimating the angular velocity of a rigid body from embedded sensors. This broad question has applications in various fields of engineering and applied science. Some specific examples are as follows. In aerospace, the deployment phase of spinning satellites starts by a detumbling maneuver during which the angular velocity is controlled in an active way until it reaches a zero value (Bošković, Li, & Mehra, 2000). The control strategy employs an estimation of this variable, in closed-loop. High velocity spinning objects are very common in ballistics. The XM25 air-burst rifle (smart-weapon) fires smart shells which estimate their rotation to determine the traveled distance (so that explosion of the projectile can be activated at any user-defined distance). Finally, the problem of angular velocity estimation can also be found in the emerging field of smart devices for sports such as the on-board football camera (Kitani, Horita, & Hideki, 2012) as it is important for athletes in many sports to train their skills to spin a ball.

In the literature, several types of methods have been proposed to address this question. On the one hand, the straightforward solution is to use a strap-down rate gyro (Titterton & Weston, 2004), which directly provides measurements of the angular velocities. However, rate gyros being relatively fragile and expensive components, prone to drift, other types of solutions are often preferred. Instead, a *two-step approach* is commonly employed. The *first step* is to determine attitude from vector measurements, i.e. on-board measurements of reference vectors being known in a fixed frame. Vector measurements play a central role in the problem of attitude determination as discussed in a recent survey (Crassidis, Markley, & Cheng, 2007). In a nutshell, when two or more independent vectors are measured with vector sensors attached to a rigid body, its attitude can be simply defined as the solution of the classic Wahba problem (Wahba, 1965) which formulates a minimization problem having the rotation matrix from a fixed frame to the body frame as unknown. The *second step* is to reconstruct angular velocities from the attitude. At any instant, full attitude information can be obtained (Bar-Itzhack, 1996; Choukroun, 2003; Shuster, 1978, 1990). In principles, once the attitude is known, angular velocity can be estimated from a time-differentiation. The survey (Bar-Itzhack, 2001) names this approach the *derivative method*. However, noise disturbs this process. To address this issue, introducing *a priori* information in the estimation process is a valuable technique to filter-out noise from the estimates. For this reason, numerous observers using Euler's equations for a rigid body have been proposed to estimate angular velocity (or angular momentum, which is equivalent) from full attitude information (Jorgensen & Gravdahl, 2011; Salcudean, 1991; Sunde, 2005; Thienel & Sanner, 2007). Besides this two-step approach, a more direct solution can be proposed. In this paper, we expose an algorithm that directly uses the vector measurements and reconstructs the angular velocity in a simple manner.

☆ The material in this paper was not presented at any conference. This paper was recommended for publication in revised form by Associate Editor Marco Lovera under the direction of Editor Toshiharu Sugie.

E-mail addresses: lionel.magnis@mines-paristech.fr (L. Magnis), nicolas.petit@mines-paristech.fr (N. Petit).

http://dx.doi.org/10.1016/j.automatica.2016.09.027
0005-1098/

The contribution of this paper is a nonlinear observer reconstructing the angular velocity of a rotating rigid body from vector measurements *directly*, namely by bypassing the relatively heavy first step of attitude estimation. Variants and extensions of this approach can be found in Magnis (2015), Magnis and Petit (2013) and Magnis and Petit (2015a,b). The proposed method allows one to estimate the angular velocity without any gyroscope. Contrary to the method presented in Oshman and Dellus (2003), it does not employ time differentiation of the measurements.

This paper is organized as follows. In Section 2, we introduce the notations and the problem statement. We analyze the attitude dynamics (rotation and Euler equations) and relate it to the measurements. In Section 3, we define a nonlinear observer with extended state and output injection. To prove its convergence, the error equation is identified as a linear time-varying (LTV) system perturbed by a linear–quadratic term. The dominant part of the LTV dynamics can be shown, by a scaling resulting from a high gain design, to generate an arbitrarily fast exponentially convergent dynamics. In turn, this property reveals instrumental to conclude on the exponential uniform convergence of the error dynamics. Illustrative simulation results are given in Section 4. Conclusions and perspectives are given in Section 5.

2. Notations and problem statement

2.1. Notations

Norms. The Euclidean norms in $\mathbf{R}^3$ and in $\mathbf{R}^9$ are denoted by $|\cdot|$. The induced norm on 9×9 matrices is denoted by $\|\cdot\|$. Namely, $\|M\| = \max_{X\in\mathbf{R}^9,\ |X|=1} |MX|$.

The cross-product matrix associated with a vector $x \in \mathbf{R}^3$ is denoted by $[x_\times]$, i.e. $\forall y \in \mathbf{R}^3,\ \ [x_\times]\, y = x \times y$. Namely,

$$[x_\times] \triangleq \begin{pmatrix} 0 & -x_3 & x_2 \\ x_3 & 0 & -x_1 \\ -x_2 & x_1 & 0 \end{pmatrix}$$

where x_1, x_2, x_3 are the coordinates of x in the standard basis of $\mathbf{R}^3$.

2.2. Problem statement

Consider a rigid body rotating with respect to an inertial frame $\mathcal{R}_i$. Note R the rotation (orthogonal) matrix representing the linear mapping from $\mathcal{R}_i$ to a body frame $\mathcal{R}_b$ attached to the rigid body, expressed in $\mathcal{R}_i$. R satisfies the differential equation

$$\dot{R} = R\,[\omega_\times] \tag{1}$$

where ω is the *angular velocity* of the rigid body expressed in the body frame. The dynamics of ω itself is governed by the famed Euler's equations (Landau & Lifchitz, 1982)

$$\dot{\omega} = J^{-1}\,(J\omega \times \omega + \tau) \tag{2}$$

where $J = \mathrm{diag}(J_1, J_2, J_3)$ is the matrix of inertia[1] and τ is the external torque applied to the rigid body.

Consider two reference vectors $\mathring{a}, \mathring{b}$ expressed in the inertial frame. Then, the expressions of a, b in the body frame at time t are

$$a(t) = R(t)^T\mathring{a}, \qquad b(t) = R(t)^T\mathring{b}. \tag{3}$$

The variables a, b are called *vector measurements*. For implementation, they can be produced by direction sensors such as e.g. accelerometers, magnetometers or Sun sensors to name a few (Magnis & Petit, 2014).

[1] Without loss of generality, we consider that the axes of $\mathcal{R}_b$ are aligned with the principal axes of inertia of the rigid body.

We now formulate some assumptions.

Assumption 1. $\mathring{a}, \mathring{b}$ are constants and linearly independent.

Assumption 2. J and τ are known.

Assumption 3. ω is bounded: $|\omega(t)| \le \omega_{\max}$ at all times.

The problem we address in this paper is the following.

Problem 1. From measurements of the type (3), find an estimate $\hat{\omega}$ of the angular velocity ω appearing in (1), assuming it satisfies (2).

Remark 1. Without loss of generality, we assume $\mathring{a}^T\mathring{b} \ge 0$ (if not, one can simply consider $-\mathring{a}$ instead of $\mathring{a}$). We denote

$$p \triangleq \mathring{a}^T\mathring{b} \ge 0.$$

Assumption 1 implies that p is constant and $p \in [0, 1)$. Note that, for all time t

$$a(t)^T b(t) = \mathring{a}^T R(t) R(t)^T \mathring{b} = \mathring{a}^T\mathring{b} = p.$$

3. Observer definition and analysis of convergence

3.1. Observer definition

From Assumption 1, we have $\frac{d}{dt}\mathring{a} = 0$. Hence, the time derivative of the measurement a is

$$\dot{a} = \dot{R}^T\mathring{a} = -[\omega_\times]\,R^T\mathring{a} = a \times \omega \tag{4}$$

and the same holds for $\dot{b} = b \times \omega$. To solve Problem 1, the main idea of the paper is to consider the reconstruction of the extended 9-dimensional state X by its estimate $\hat{X}$

$$X = \begin{pmatrix} a^T & b^T & \omega^T \end{pmatrix}^T, \qquad \hat{X} = \begin{pmatrix} \hat{a}^T & \hat{b}^T & \hat{\omega}^T \end{pmatrix}^T.$$

The state is governed by

$$\dot{X} = \begin{pmatrix} a \times \omega \\ b \times \omega \\ E(\omega) + J^{-1}\tau \end{pmatrix} \tag{5}$$

and the following observer is proposed

$$\dot{\hat{X}} = \begin{pmatrix} a \times \hat{\omega} - \alpha k(\hat{a} - a) \\ b \times \hat{\omega} - \alpha k(\hat{b} - b) \\ E(\hat{\omega}) + J^{-1}\tau + k^2\left(a \times \hat{a} + b \times \hat{b}\right) \end{pmatrix} \tag{6}$$

where $\alpha \in (0, 2\sqrt{1-p})$ and $k > 0$ are constant (tuning) parameters. Denote

$$\tilde{X} \triangleq X - \hat{X} \triangleq \begin{pmatrix} \tilde{a}^T & \tilde{b}^T & \tilde{\omega}^T \end{pmatrix}^T \tag{7}$$

the error state. We have

$$\dot{\tilde{X}} = \begin{pmatrix} -\alpha k I & 0 & [a_\times] \\ 0 & -\alpha k I & [b_\times] \\ k^2\,[a_\times] & k^2\,[b_\times] & 0 \end{pmatrix} \tilde{X} + \begin{pmatrix} 0 \\ 0 \\ E(\omega) - E(\hat{\omega}) \end{pmatrix}. \tag{8}$$

In Section 3.4 we will exhibit, for each value $0 < \alpha < (2\sqrt{1-p})$, a threshold value k^* such that for $k > k^*$, $\tilde{X}$ converges locally uniformly exponentially to zero.

3.2. Preliminary change of variables and properties

The study of the dynamics (8) employs a preliminary change of coordinates. Denote

$$Z \triangleq \begin{pmatrix} \tilde{a}^T & \tilde{b}^T & \dfrac{\tilde{\omega}}{k}^T \end{pmatrix}^T \tag{9}$$

yielding a reformulation of (8)

$$\dot{Z} = kA(t)Z + \begin{pmatrix} 0 & 0 & \dfrac{E(\omega)^T - E(\hat{\omega})^T}{k} \end{pmatrix}^T \tag{10}$$

with

$$A(t) \triangleq \begin{pmatrix} -\alpha I & 0 & [a(t)_\times] \\ 0 & -\alpha I & [b(t)_\times] \\ [a(t)_\times] & [b(t)_\times] & 0 \end{pmatrix} \tag{11}$$

which we will analyze as an ideal linear time-varying (LTV) system

$$\dot{Z} = kA(t)Z \tag{12}$$

disturbed by the input term

$$\xi \triangleq \begin{pmatrix} 0 & 0 & \dfrac{E(\omega)^T - E(\hat{\omega})^T}{k} \end{pmatrix}^T. \tag{13}$$

The idea is that for sufficiently large values of k, the rate of convergence of (12) will ensure stability of system (10). We start by upper-bounding $A(t)$ and the disturbance (13).

Proposition 1 (*Bound on the Unforced LTV System*)**.** *$A(t)$ defined in (11) is upper-bounded by*

$$A_{\max} \triangleq \max\left(\sqrt{2+2\alpha^2}, \sqrt{3+\alpha^2}\right).$$

Proof. Let $Y \in \mathbf{R}^9$ such that $|Y| = 1$. For convenience, denote

$$Y = \begin{pmatrix} Y_1^T & Y_2^T & Y_3^T \end{pmatrix}^T$$

with $Y_i \in \mathbf{R}^3$. One has

$$\begin{aligned} |A(t)Y|^2 &= |-\alpha Y_1 + a \times Y_3|^2 + |-\alpha Y_2 + b \times Y_3|^2 \\ &\quad + |a \times Y_1 + b \times Y_2|^2 \\ &\le (1+\alpha^2)\left(|Y_1|^2 + |a \times Y_3|^2 + |Y_2|^2 + |b \times Y_3|^2\right) \\ &\quad + 2\left(|a \times Y_1|^2 + |b \times Y_2|^2\right) \\ &\le \max\left(2+2\alpha^2, 3+\alpha^2\right)|Y|^2 = A_{\max}^2. \end{aligned}$$

Hence, $\|A(t)\| = \max_{|Y|=1} |A(t)Y| \le A_{\max}$.

Proposition 2 (*Bound on the Disturbance*)**.** *For any Z, ξ is bounded by*

$$|\xi| \le \sqrt{2}\omega_{\max}|Z| + k|Z|^2. \tag{14}$$

Proof. We have

$$|\xi| = \frac{1}{k}|E(\omega) - E(\hat{\omega})|$$

with, due to the quadratic nature of $E(\cdot)$,

$$E(\omega) - E(\hat{\omega}) = J^{-1}\left(J\tilde{\omega} \times \omega + J\omega \times \tilde{\omega} - J\tilde{\omega} \times \tilde{\omega}\right)$$

Using $J = \mathrm{diag}(J_1, J_2, J_3)$, we have

$$J^{-1}\left(J\tilde{\omega} \times \omega\right) = \begin{pmatrix} \dfrac{1}{J_1}(J_2\tilde{\omega}_2\omega_3 - J_3\omega_2\tilde{\omega}_3) \\ \dfrac{1}{J_2}(J_3\tilde{\omega}_3\omega_1 - J_1\omega_3\tilde{\omega}_1) \\ \dfrac{1}{J_3}(J_1\tilde{\omega}_1\omega_2 - J_2\omega_1\tilde{\omega}_2) \end{pmatrix}.$$

Using similar expressions for $J^{-1}(J\omega \times \tilde{\omega})$ and $J^{-1}(J\tilde{\omega} \times \tilde{\omega})$ yields

$$\begin{aligned} E(\omega) - E(\hat{\omega}) &= \begin{pmatrix} \dfrac{J_2 - J_3}{J_1}(\omega_2\tilde{\omega}_3 + \tilde{\omega}_2\omega_3) \\ \dfrac{J_3 - J_1}{J_2}(\omega_3\tilde{\omega}_1 + \tilde{\omega}_3\omega_1) \\ \dfrac{J_1 - J_2}{J_3}(\omega_1\tilde{\omega}_2 + \tilde{\omega}_1\omega_2) \end{pmatrix} - \begin{pmatrix} \dfrac{J_2 - J_3}{J_1}\tilde{\omega}_2\tilde{\omega}_3 \\ \dfrac{J_3 - J_1}{J_2}\tilde{\omega}_3\tilde{\omega}_1 \\ \dfrac{J_1 - J_2}{J_3}\tilde{\omega}_1\tilde{\omega}_2 \end{pmatrix} \\ &\triangleq \delta_1 - \delta_2. \end{aligned}$$

As J_1, J_2, J_3 are the main moments of inertia of the rigid body, we have (Landau & Lifchitz, 1982, Section 32, 9) $J_i \le J_j + J_k$ for all permutations i, j, k and hence

$$\left|\frac{J_2 - J_3}{J_1}\right|, \quad \left|\frac{J_3 - J_1}{J_2}\right|, \quad \left|\frac{J_1 - J_2}{J_3}\right| \quad \le 1.$$

As a straightforward consequence $|\delta_2| \le |\tilde{\omega}|^2$. Moreover, by the Cauchy–Schwarz inequality

$$(\omega_2\tilde{\omega}_3 + \tilde{\omega}_2\omega_3)^2 \le (\omega_2^2 + \omega_3^2)(\tilde{\omega}_2^2 + \tilde{\omega}_3^2) \le (\omega_2^2 + \omega_3^2)|\tilde{\omega}|^2.$$

Using similar inequalities for all the coordinates of δ_1 yields

$$|\delta_1|^2 \le 2|\omega|^2|\tilde{\omega}|^2 \le 2\omega_{\max}^2|\tilde{\omega}|^2.$$

Hence,

$$\begin{aligned} |\xi| \le \frac{|\delta_1| + |\delta_2|}{k} &\le \sqrt{2}\omega_{\max}\left|\frac{\tilde{\omega}}{k}\right| + k\left|\frac{\tilde{\omega}}{k}\right|^2 \\ &\le \sqrt{2}\omega_{\max}|Z| + k|Z|^2. \end{aligned}$$

3.3. Analysis of the LTV dynamics $\dot{Z} = kA(t)Z$

We will now use a result on the exponential stability of LTV systems. The claim of Hill and Ilchmann (2011, Theorem 2.1), which is instrumental in the proof of the next result, is as follows: consider a LTV system $\dot{Z} = M(t)Z$ such that: (i) $M(\cdot)$ is l-Lipschitz, with $l > 0$, (ii) there exist $K \ge 1$, $c \ge 0$ such that for any t and any $s \ge 0$, $\left\|e^{M(t)s}\right\| \le Ke^{-cs}$ (frozen-time exponential stability). Then, for any t_0, Z_0, the solution of $\dot{Z} = M(t)Z$ with initial condition $Z(t_0) = Z_0$ satisfies, for any $t \ge t_0$,

$$|Z(t)| \le Ke^{(\sqrt{Kl\ln K} - c)(t - t_0)}|Z_0|.$$

Using this result, we will show that the convergence of (12) can be tailored by choosing k to arbitrarily increase the rate of convergence, while keeping the overshoot constant.

Theorem 1. *Let $\alpha \in (0, 2\sqrt{1-p})$ be fixed. There exists a continuous function $\gamma(k)$ satisfying*

$$\lim_{k \to +\infty} \gamma(k) = +\infty$$

such that the solution of (12) satisfies

$$|Z(t)| \le Ke^{-\gamma(k)(t - t_0)}|Z(t_0)|$$

with

$$K \triangleq \sqrt{\frac{1 + \frac{\alpha}{2\sqrt{1-p}}}{1 - \frac{\alpha}{2\sqrt{1-p}}}} \tag{15}$$

for any initial condition t_0, $Z(t_0)$ and any $t \ge t_0$.

Proof. Consider any fixed value of t. We start by studying the frozen-time matrix $A(t)$. Denote

$$\mu \triangleq \sqrt{8(1 - p^2)}.$$

Introduce the following (time-varying) matrices

$$P_1 = \begin{pmatrix} a & 0 & \dfrac{b-pa}{\sqrt{2(1-p^2)}} \\ 0 & b & \dfrac{a-pb}{\sqrt{2(1-p^2)}} \\ 0 & 0 & 0 \end{pmatrix}$$

$$P_2 = \frac{1}{\mu}\begin{pmatrix} 2(pa-b) & 0 \\ 2(a-pb) & 0 \\ \alpha\, a\times b & -\sqrt{8-\alpha^2}\, a\times b \end{pmatrix}$$

$$P_3 = \frac{1}{\mu}\begin{pmatrix} 2a\times b & 0 \\ 2a\times b & 0 \\ \alpha(b-a) & \sqrt{4(1+p)-\alpha^2}(a-b) \end{pmatrix}$$

$$P_4 = \frac{1}{\mu}\begin{pmatrix} 2a\times b & 0 \\ -2a\times b & 0 \\ \alpha(a+b) & -\sqrt{4(1-p)-\alpha^2}(a+b) \end{pmatrix}$$

and

$$P = (P_1|P_2|P_3|P_4) \in \mathbf{R}^{9\times 9}.$$

We have

$$P^{-1}A(t)P = \begin{pmatrix} M_1 & 0 & 0 & 0 \\ 0 & M_2 & 0 & 0 \\ 0 & 0 & M_3 & 0 \\ 0 & 0 & 0 & M_4 \end{pmatrix}$$

with

$$M_1 = -\alpha I, \qquad M_i = \frac{1}{2}\begin{pmatrix} -\alpha & -\sqrt{\alpha_i-\alpha^2} \\ \sqrt{\alpha_i-\alpha^2} & -\alpha \end{pmatrix}$$

for $i = 2, 3, 4$ with

$$\alpha_2 \triangleq 2\sqrt{2} \;>\; \alpha_3 \triangleq 2\sqrt{1+p} \;\geq\; \alpha_4 \triangleq 2\sqrt{1-p} \;>\; \alpha.$$

For all $s \geq 0$

$$\left\|e^{A(t)s}\right\| \leq \|P\|\left\|P^{-1}\right\| e^{-\frac{\alpha}{2}s}.$$

Moreover

$$\|P\|\left\|P^{-1}\right\| = \sqrt{\frac{\lambda_{\max}(P^TP)}{\lambda_{\min}(P^TP)}}$$

where $\lambda_{\max}(\cdot)$, $\lambda_{\min}(\cdot)$ respectively designate the maximum and minimum eigenvalues. Besides,

$$P^TP = \begin{pmatrix} I & 0 & 0 & 0 \\ 0 & Q_2 & 0 & 0 \\ 0 & 0 & Q_3 & 0 \\ 0 & 0 & 0 & Q_4 \end{pmatrix}$$

with, for $i = 2, 3, 4$

$$Q_i = \begin{pmatrix} 1+\dfrac{\alpha^2}{\alpha_i^2} & \dfrac{\alpha}{\alpha_i}\sqrt{1-\dfrac{\alpha}{\alpha_i}} \\ \dfrac{\alpha}{\alpha_i}\sqrt{1-\dfrac{\alpha}{\alpha_i}} & 1-\dfrac{\alpha^2}{\alpha_i^2} \end{pmatrix}$$

yielding the eigenvalues

$$\mathrm{eig}(P^TP) = \left\{1, 1\pm\frac{\alpha}{2\sqrt{2}}, 1\pm\frac{\alpha}{2\sqrt{1+p}}, 1\pm\frac{\alpha}{2\sqrt{1-p}}\right\}.$$

Thus, for all $s \geq 0$

$$\|e^{A(t)s}\| \leq Ke^{-\frac{\alpha}{2}s}$$

with

$$K = \sqrt{\frac{\lambda_{\max}(P^TP)}{\lambda_{\min}(P^TP)}} = \sqrt{\frac{1+\frac{\alpha}{2\sqrt{1-p}}}{1-\frac{\alpha}{2\sqrt{1-p}}}}.$$

Let the tuning gain $k > 0$ be fixed. The scaled matrix $kA(\cdot)$ satisfies

$$\|e^{kA(t)s}\| \leq Ke^{-\frac{k\alpha}{2}s}, \quad \forall t,\ \forall s \geq 0.$$

Moreover, for any $Y \in \mathbf{R}^9$ and any $t, s \in \mathbf{R}$, one has

$$(kA(s)-kA(t))Y = k\int_t^s \dot{A}(u)du\, Y$$

$$= k\begin{pmatrix} \int_t^s a(u)\times\omega(u)du\, Y_3 \\ \int_t^s b(u)\times\omega(u)du\, Y_3 \\ \int_t^s a(u)\times\omega(u)du\, Y_1 + \int_t^s b(u)\times\omega(u)du\, Y_2 \end{pmatrix}.$$

Hence

$$|(kA(s)-kA(t))Y|^2 \leq 2\omega_{\max}^2 k^2|s-t|^2|Y|^2.$$

Thus, $kA(\cdot)$ is kL-Lipschitz with

$$L \triangleq \sqrt{2}\omega_{\max}. \tag{16}$$

We now apply Hill and Ilchmann (2011, Theorem 2.1). For any t_0 and any Z_0, the solution of (12) with initial condition $Z(t_0) = Z_0$ satisfies for all $t \geq t_0$

$$|Z(t)| \leq Ke^{\left(\sqrt{kKL\ln K}-\frac{k\alpha}{2}\right)(t-t_0)}|Z_0|$$

which concludes the proof with

$$\gamma(k) \triangleq \frac{k\alpha}{2} - \sqrt{kKL\ln K}. \tag{17}$$

Remark 2. Additionally, one can note that: (i) $\gamma(k) > 0 \Leftrightarrow k > \frac{4KL\ln K}{\alpha^2}$ in which case Theorem 1 ensures exponential stability of system (12), (ii) $\gamma(\cdot)$ is strictly increasing for $k > \frac{4KL\ln K}{\alpha^2}$, (iii) in the case where $p = 1$, which does not fall under the assumptions of this paper, the preceding analysis would not hold. First, the interval $(0, 2\sqrt{1-p})$ would be empty. Second, $\mu = 0$ and the matrices P_i would not be well defined.

3.4. Convergence of the observer

Define r as

$$r(k) \triangleq \frac{1}{\sqrt{A_{\max}}K^3}\left(1-\frac{K^2\sqrt{2}\omega_{\max}}{\gamma(k)}\right)\left(\frac{\gamma(k)}{k}\right)^{\frac{3}{2}} \tag{18}$$

and k^* as

$$k^* = \frac{\left(\sqrt{\ln K}+\sqrt{\ln K + 2\alpha K}\right)^2}{\alpha^2}\sqrt{2}K\omega_{\max} > 0. \tag{19}$$

The following holds

Proposition 3. *$r(k) > 0$ if and only if $k > k^*$*

Proof. A simple rewriting of $r(k) > 0$ yields, successively,

$$r(k) > 0 \Leftrightarrow \gamma(k) > K^2\sqrt{2}\omega_{\max} = K^2L$$

$$\Leftrightarrow \frac{\alpha}{2}k - \sqrt{LK\ln K}\sqrt{k} - K^2L > 0$$

$$\Leftrightarrow \sqrt{k} > \frac{\sqrt{LK\ln K}+\sqrt{LK\ln K + 2\alpha LK^2}}{\alpha} = \sqrt{k^*}$$

which concludes the proof.

We can now state the main result of the paper.

Theorem 2 (*Solution to Problem 1*). *For any $\alpha \in (0, 2\sqrt{1-p})$, there exists k^* defined by (19) such that for $k > k^*$, the observer (6) defines an error dynamics (8) for which the equilibrium 0 is locally uniformly exponentially stable. The basin of attraction of this equilibrium contains the ellipsoid*

$$\left\{\tilde{X}(t_0),\ |\tilde{a}(t_0)|^2 + |\tilde{b}(t_0)|^2 + \frac{|\tilde{\omega}(t_0)|^2}{k^2} < r(k)^2\right\} \tag{20}$$

where $r(k)$ is defined by (18).

Proof. Let $k > k^*$. Consider the candidate Lyapunov function

$$V(t,Z) \triangleq Z^T \left(\int_t^{+\infty} \phi(\tau,t)^T \phi(\tau,t) d\tau\right) Z$$

where ϕ is the transition matrix of system (12). Let (t, Z) be fixed. From Proposition 1, $kA(\cdot)$ is bounded by $kA_{\max}$. Thus (see for example Khalil, 2000, Theorem 4.12)

$$V(t,Z) \geq \frac{1}{2kA_{\max}} |Z|^2 \triangleq c_1 |Z|^2 \triangleq W_1(Z).$$

Moreover, Theorem 1 implies that for all $\tau \geq t$

$$|\phi(\tau,t)Z| \leq K e^{-\gamma(k)(\tau-t)} |Z|$$

which gives

$$V(t,Z) \leq K^2 \int_t^{+\infty} e^{-2\gamma(k)(\tau-t)} d\tau |Z|^2 = \frac{K^2}{2\gamma(k)} |Z|^2$$
$$\triangleq c_2 |Z|^2 \triangleq W_2(Z).$$

By construction, V satisfies

$$\frac{\partial V}{\partial t}(t,Z) + \frac{\partial}{\partial Z} V(t,Z) kA(t) Z = -|Z|^2.$$

Hence, the derivative of V along the trajectories of (10) is $\frac{d}{dt}V(t,Z) = -|Z|^2 + \frac{\partial V}{\partial Z}(t,Z)\,\xi$. Using

$$\left|\frac{\partial}{\partial Z} V(t,Z)\right| = 2\left|\int_t^{+\infty} \phi(\tau,t)^T \phi(\tau,t) d\tau Z\right| \leq \frac{K^2}{\gamma(k)} |Z|$$

together with inequality (14) yields

$$\left|\frac{\partial V}{\partial Z}(t,Z)\,\xi\right| \leq \frac{K^2}{\gamma(k)} \left(\sqrt{2}\omega_{\max} |Z|^2 + k|Z|^3\right).$$

Hence

$$\frac{d}{dt} V(t,Z) \leq -|Z|^2 \left(1 - \frac{K^2\sqrt{2}\omega_{\max}}{\gamma(k)} - \frac{kK^2}{\gamma(k)} |Z|\right)$$
$$\triangleq -W_3(Z).$$

As $k > k^*$, we have $1 - \frac{K^2\sqrt{2}\omega_{\max}}{\gamma(k)} > 0$. We proceed as in Khalil (2000, Theorem 4.9). If the initial condition of (10) satisfies $|Z(t_0)| < r(k)$, or equivalently

$$|Z(t_0)| < \frac{\gamma(k)}{kK^2} \left(1 - \frac{K^2\sqrt{2}\omega_{\max}}{\gamma(k)}\right) \times \sqrt{\frac{c_1}{c_2}}$$

then $W_3(Z(t_0)) > 0$ and, while $W_3(Z(t)) > 0$, $Z(\cdot)$ remains bounded by

$$|Z(t)|^2 \leq \frac{V(t)}{c_1} \leq \frac{V(t_0)}{c_1} \leq \frac{c_2}{c_1} |Z(t_0)|^2$$

which shows that

$$W_3(Z) \geq \left(1 - \frac{K^2\sqrt{2}\omega_{\max}}{\gamma(k)} - \frac{kK^2}{\gamma(k)} \sqrt{\frac{c_2}{c_1}} |Z(t_0)|\right) |Z|^2$$
$$\triangleq c_3 |Z|^2$$

so that

$$\frac{d}{dt} V(t, Z(t)) \leq -c_3 |Z(t)|^2 \leq -\frac{c_3}{c_2} V(t, Z(t))$$

and in the end

$$|Z(t)|^2 \leq \frac{1}{c_1} e^{-\frac{c_3}{c_2}(t-t_0)} V(t_0, Z(t_0))$$
$$\leq \frac{c_2}{c_1} e^{-\frac{c_3}{c_2}(t-t_0)} |Z(t_0)|^2.$$

This shows that the 0 equilibrium of (10) is locally uniformly exponentially stable and that its basin of attraction contains the ball of equation

$$|Z(t_0)|^2 < r(k)^2.$$

Using (9) to go back to the $\tilde{a}, \tilde{b}, \tilde{\omega}$ coordinates allows one to deduce that the basin of attraction contains the ellipsoid (20).

Remark 3. The limitations imposed on $\tilde{a}(t_0)$ and $\tilde{b}(t_0)$ in (20) are not truly restrictive, as the actual values $a(t_0)$, $b(t_0)$ are assumed known, so the observer may be initialized with $\tilde{a}(t_0) = 0$, $\tilde{b}(t_0) = 0$. What matters is that the error on the unknown quantity $\omega(t_0)$ can be large in practice. Interestingly, when k goes to infinity $r(k)$ tends to the limit $\frac{1}{\sqrt{A_{\max}K^3}} \left(\frac{\alpha}{2}\right)^{\frac{3}{2}} > 0$ and arbitrarily large initial error $\tilde{\omega}(t_0)$ is thus allowed from (20).

Remark 4. The threshold k^* depends linearly on $\omega_{\max}$, which gives helpful hint in the tuning of observer (6).

Remark 5. As $\frac{c_3}{c_2}$ goes to infinity with k, the convergence rate is arbitrary fast for k large enough.

4. Simulation results

In the simulations reported here, we consider that the rigid body is a parallelepiped of size $10 \times 10 \times 20$ [cm^3] having a homogeneously distributed mass of 2 [kg]. The resulting moments of inertia are

$$J_1 = 88 \text{ [kg cm}^2], \qquad J_2 = 88 \text{ [kg cm}^2], \qquad J_3 = 33 \text{ [kg cm}^2].$$

No torque is applied to the system, which is thus in free-rotation.

4.1. Sensitivity to parameters

We illustrate the dependence of the observer with respect to three parameters: (i) p which quantifies the linear independence of $(\mathring{a}, \mathring{b})$, (ii) $\omega_{\max}$ the maximal rotation rate of the rigid body, (iii) the tuning gain k. To this end, we chose the reference vectors as

$$\mathring{a} = \begin{pmatrix}1 & 0 & 0\end{pmatrix}^T, \qquad \mathring{b} = \begin{pmatrix}p & \sqrt{1-p^2} & 0\end{pmatrix}^T.$$

For sake of accuracy in the implementation, reference dynamics (5) and state observer (6) were simulated using Runge–Kutta 4 method with sample period 0.1 [s] for various values of p and $\omega(0)$ and with $\alpha = \sqrt{1-p}$. Additive white Gaussian noise with standard deviation $\sigma_a = 0.025$ [Hz$^{-\frac{1}{2}}$] (respectively $\sigma_b = 0.02$ [Hz$^{-\frac{1}{2}}$]) was added to each measurement coordinate of a (respectively b). Typical measurements are given in Fig. 1.

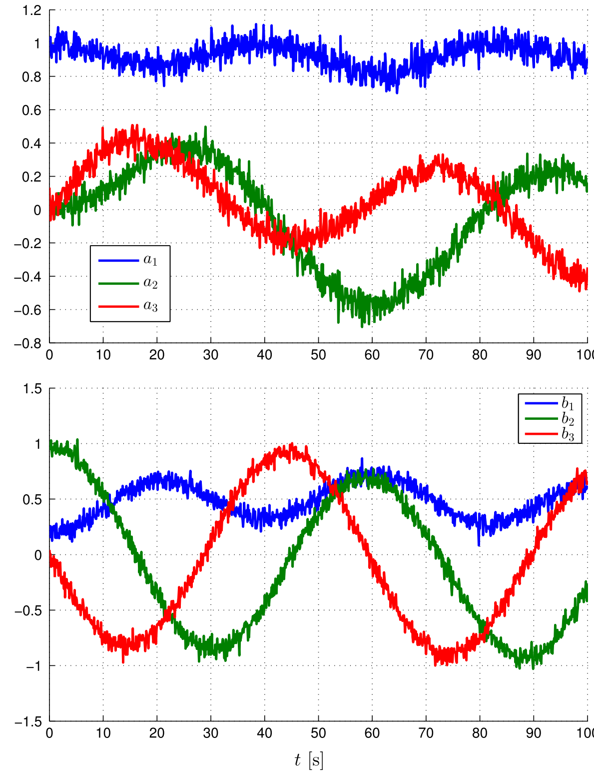

Fig. 1. Vector measurements: a (top, three coordinates) and b (bottom, three coordinates).

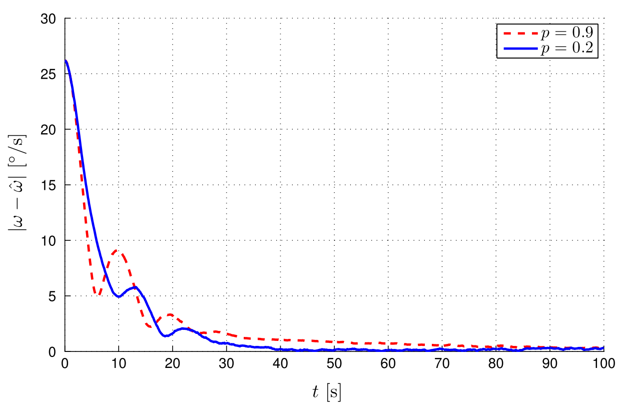

Fig. 2. $k = 0.25$, $\omega_{\max} = 6$ [°/s]. The rate of convergence degrades when p increases.

Fig. 2 shows the influence of p. When p gets close to 1, the rate of convergence is decreased. This was to be expected. To the limit, when $p \to 1$, all the matrices $A(t)$ become singular and the proof of convergence cannot be applied anymore. Note that the measurement noise is smoothly filtered by the observer, thanks to the relatively low value of the gain k.

In Fig. 3, we report the behavior of the observer for increasing values of $\omega_{\max}$. The faster the rotation, the slower the convergence. A faster convergence can be achieved by increasing the gain k. This increases the sensitivity to noise, as represented in Fig. 4.

4.2. Orbital trajectory

We now challenge Assumption 1. We investigate the behavior of the observer in the case where $\mathring{b}$ is time-varying, which might happen in real-life applications. In the following, the rigid body is a satellite in orbit. It is rotating about its center of gravity which trajectory is an orbit. The two reference vectors are the Sun direction $\mathring{a}$ and the normalized magnetic field $\mathring{b}$. The satellite is equipped with 6 Sun sensors providing at all times a measure of the Sun direction y_a in a Sun sensor frame $\mathcal{R}_s$, and 3 magnetometers able to measure the normalized magnetic field y_b in a magnetometer frame $\mathcal{R}_m$. It shall be noted that the sensor frames $\mathcal{R}_s$ need not coincide with $\mathcal{R}_m$ and can also differ from the body frame $\mathcal{R}_b$ (defined along the principal axes of inertia) through a constant rotation $R_{m,b}$, respectively $R_{s,b}$. With these notations, we have

$$a = R_{m,b}^T y_a, \qquad b = R_{s,b}^T y_b$$

which is a simple change of coordinates of the measurements.

We simulate 50 min (approx. half a period) of the trajectory of the satellite on a circular orbit with altitude 765 [km] and

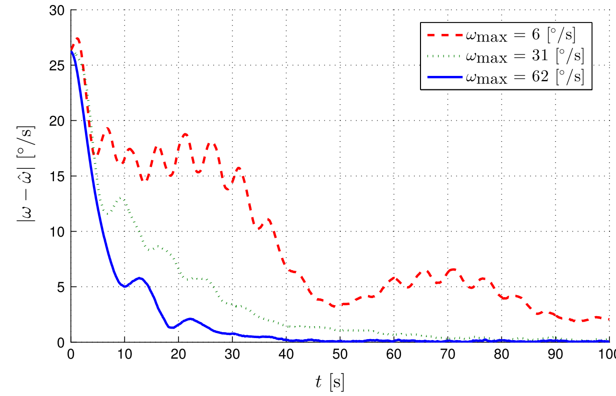

Fig. 3. $k = 0.25$, $p = 0.2$. Impact of $\omega_{\max}$ on the convergence rate.

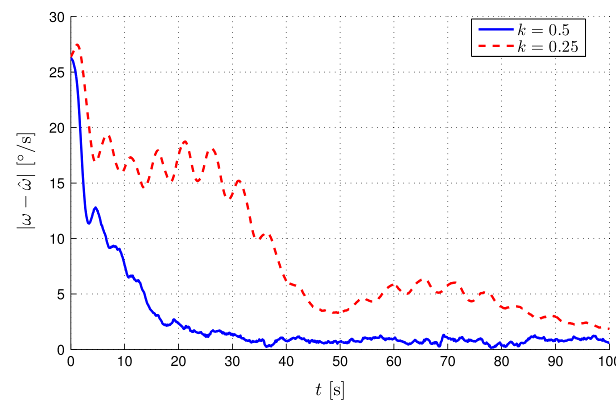

Fig. 4. $\omega_{\max} = 62$ [°/s], $p = 0.2$. When k increases, the convergence is faster but the measurement noise filtering degrades.

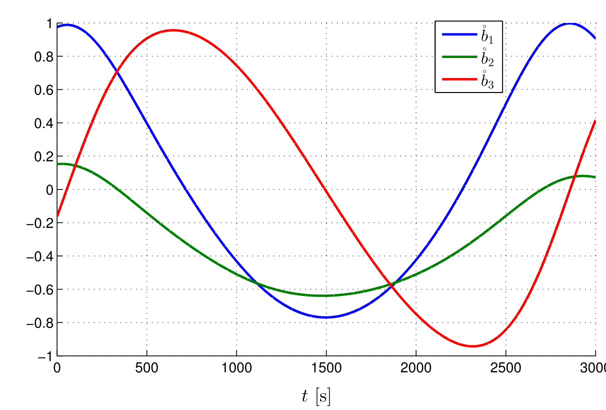

Fig. 5. Variations of the normalized reference magnetic field along the orbit.

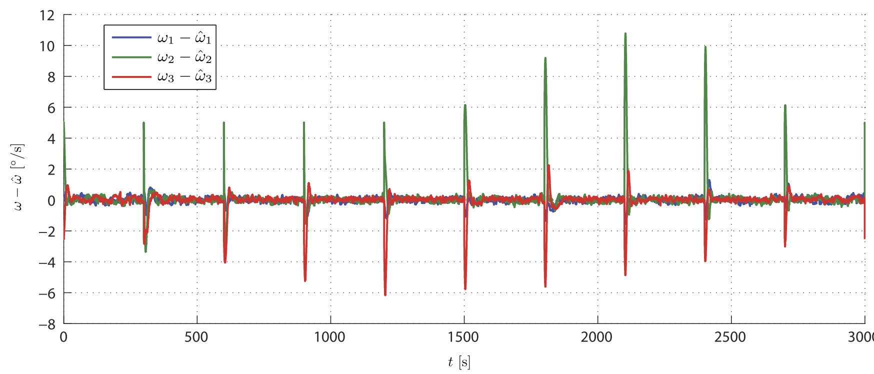

Fig. 6. $k = 0.25$. Observer performance along the orbit. The residual error is due to the variation of $\mathring{b}$ and the measurement noise. An artificial reset is made every 300 [s].

inclination 30 [°] with respect to a polar orbit. Leaving out the consideration of Earth shadowing (which does not occur for this half orbit), the Sun direction $\mathring{a}$ is considered as constant. In the simulation its value is

$$\mathring{a} = (0.3977 \quad 0.3445 \quad 0.1989)^T$$

This is not the case for the normalized magnetic field $\mathring{b}$ which varies significantly with the latitude. As a result, the state model (5) is not valid. To accurately simulate the values of $b(t)$, we compute the full rotation dynamics (1)–(2)[2] and use the measurements Eq. (3). $\mathring{b}$ is determined by the position of the satellite using the IGRF12 model. Its values are reported in Fig. 5. Additive white Gaussian noise with standard deviation 0.02 [$\mathrm{Hz}^{-\frac{1}{2}}$] was added to each coordinate of a, b. Again, we use a Runge–Kutta 4 method with sampling period 0.1 [s]. The initial condition on ω is

$$\omega(0) = (0 \;\; 5 \;\; -2.5)^T \; [°/\mathrm{s}].$$

The performance of the observer is represented in Fig. 6. An artificial reset is performed every 300 [s] to stress the convergence properties of the error. As can be expected the convergence rate and the peaking depend on the initial time, hence on the value of $\mathring{b}$. However, the variations of these convergence parameters remain small. A residual error of about 0.3 [°/s] remains on each coordinate of $\omega - \hat{\omega}$. This is partly due to measurement noise and partly to the fact that $\mathring{b}$ varies with time. In this simulation, the contribution of those two phenomenon to the error are of similar magnitude. With less noisy sensors, it would be possible to increase the gain k further to reduce the sum of these two contributions to the error.

5. Conclusions and perspectives

A new method to estimate the angular velocity of a rigid body has been proposed in this article. The method uses on-board measurements of constant and independent vectors. The estimation algorithm is a nonlinear observer which is very simple to implement and induces a very limited computational burden. At this stage, an interesting (but still preliminary) conclusion is that, in the cases considered here, rate gyros could be replaced with an estimation software employing cheap, rugged and resilient sensors. In fact, any set of sensors producing vector measurements such as e.g., Sun sensors, magnetometers, could constitute one such alternative. Assessing the feasibility of this approach requires further investigations including experiments.

More generally, this observer should be considered as a first element of a class of estimation methods which can be developed to address several cases of practical interest. In particular, the introduction of noise in the measurement and uncertainty on the input torque (assumed here to be known) will require extensions such as optimal filtering to treat more general cases. White or colored noises will be good candidates to model these elements. Also, slow variations of the reference vectors $\mathring{a}$, $\mathring{b}$ should deserve particular care, because such drifts naturally appear in some cases. For example,Earth's magnetic field measured on-board satellites varies according to the position along the orbit.

On the other hand, one can also consider that this method can be useful for other estimation tasks. Among the possibilities are the estimation of the inertia J matrix which we believe is possible from the measurements considered here. This could be of interest for the recently considered task of space debris removal (Bonnal, Ruault, & Desjean, 2013).

Finally, recent attitude estimation techniques have favored the use of vector measurements *together* with rate gyros measurements as inputs. Among these approaches, one can find Extended Kalman Filters (EKF)-like algorithms e.g. Choukroun, Bar-Itzhack, and Oshman (2006), Choukroun, Weiss, Bar-Itzhack, and Oshman (2012) and Schmidt, Ravandoor, Kurz, Busch, and Schilling (2008), nonlinear observers (Grip, Fossen, Johansen, & Saberi, 2012; Mahony, Hamel, & Pflimlin, 2008; Martin & Salaün, 2010; Tayebi, Roberts, & Benallegue, 2011; Trumpf, Mahony, Hamel, & Lageman, 2012; Vasconcelos, Silvestre, & Oliveira, 2008), Wahba-based filtering, unscented Kalman filtering, particle filtering. This contribution suggests that, here also, the rate gyros could be replaced with more in-depth analysis of the vector measurements.

[2] For computational efficiency, we used the standard quaternion parametrization of R to simulate (1).

References

Bar-Itzhack, I. Y. (1996). REQUEST - a new recursive algorithm for attitude determination. In *Proceedings of the national technical meeting of the institude of navigation* (pp. 699–706).

Bar-Itzhack, I. Y. (2001). Classification of algorithms for angular velocity estimation. *Journal of Guidance, Control, and Dynamics*, *24*(2), 214–218.

Bošković, J. D., Li, S.-M., & Mehra, R. K. (2000). A globally stable scheme for spacecraft control in the presence of sensor bias. In *Proceedings of the IEEE aersopace conference* (pp. 505–511).

Bonnal, C., Ruault, J.-M., & Desjean, M.-C. (2013). Active debris removal: Recent progress and current trends. *Acta Astronautica*, *85*, 51–60.

Choukroun, D. (2003). *Novel methods for attitude determination using vector observations*. (Ph.D. thesis), Technion.

Choukroun, D., Bar-Itzhack, I. Y., & Oshman, Y. (2006). Novel quaternion Kalman filter. *IEEE Transactions on Aerospace and Electronic Systems*, *42*(1), 174–190.

Choukroun, D., Weiss, H., Bar-Itzhack, I. Y., & Oshman, Y. (2012). Quaternion estimation from vector observations using a matrix Kalman filter. *IEEE Transactions on Aerospace and Electronic Systems*, *48*(4).

Crassidis, J. L., Markley, F. L., & Cheng, Y. (2007). Survey of nonlinear attitude estimation methods. *Journal of Guidance, Control, and Dynamics*, *30*(1), 12–28.

Grip, H. F., Fossen, T. I., Johansen, T. A., & Saberi, A. (2012). Attitude estimation using biased gyro and vector measurements with time-varying reference vectors. *IEEE Transactions on Automatic Control*, *57*(5), 1332–1338.

Hill, A. T., & Ilchmann, A. (2011). Exponential stability of time-varying linear systems. *IMA Journal of Numerical Analysis*, *31*, 865–885.

Jorgensen, U., & Gravdahl, J. T. (2011). Observer based sliding mode attitude control: Theoretical and experimental results. *Modeling, Identification and Control*, *32*(3), 113–121.
Khalil, H. K. (2000). *Nonlinear systems* (3rd ed.). Pearson Education.
Kitani, K. M., Horita, K., & Hideki, K. (2012). Ballcam! Dynamic view synthesis from spinning cameras. In *ACM symposium on user interface software and technology, UIST*.
Landau, L., & Lifchitz, E. (1982). *Mechanics* (4th ed.). Moscou: MIR.
Magnis, L. (2015). *Estimation of angular rate from direction sensors*. (Ph.D. thesis), MINES ParisTech.
Magnis, L., & Petit, N. (2013). Rotation estimation for a satellite from sun sensors. In *Control conference (ECC), 2013 European* (pp. 852–859). IEEE.
Magnis, L., & Petit, N. (2014). Estimation of 3D rotation for a satellite from Sun sensors. In *Proceedings of the 19th IFAC world congress* (pp. 10004–10011).
Magnis, L., & Petit, N. (2015a). Angular velocity nonlinear observer from single vector measurements. *IEEE Transactions on Automatic Control*, *PP*(99), 1–1.
Magnis, L., & Petit, N. (2015b). *Gyroless ball: estimation of angular velocity without gyroscope. Research Report*. MINES ParisTech.
Mahony, R., Hamel, T., & Pflimlin, J. M. (2008). Nonlinear complementary filters on the special orthogonal group. *IEEE Transactions on Automatic Control*, *53*(5), 1203–1218.
Martin, P., & Salaün, E. (2010). Design and implementation of a low-cost observer-based attitude and heading reference system. *Control Engineering Practice*, *18*, 712–722.
Oshman, Y., & Dellus, F. (2003). Spacecraft angular velocity estimation using sequential observations of a single directional vector. *Journal of Spacecraft and Rockets*, *40*(2), 237–247.
Salcudean, S. (1991). A globally convergent angular velocity observer for rigid body motion. *IEEE Transactions on Automatic Control*, *36*(12), 1493–1497.
Schmidt, M., Ravandoor, K., Kurz, O., Busch, S., & Schilling, K. (2008). Attitude determination for the Pico-Satellite UWE-2. In *Proceedings of the 17th IFAC world congress* (pp. 14036–14041).
Shuster, M. D. (1978). Approximate algorithms for fast optimal attitude computation. In *Proceedings of the AIAA guidance and control conference* (pp. 88–95).
Shuster, M. D. (1990). Kalman filtering of spacecraft attitude and the QUEST model. *The Journal of the Astronautical Sciences*, *38*(3), 377–393.
Sunde, B. O. (2005). *Sensor modelling and attitude determination for micro-satellites*. (Master's thesis), NTNU.
Tayebi, A., Roberts, A., & Benallegue, A. (2011). Inertial measurements based dynamic attitude estimation and velocity-free attitude stabilization. In *American control conference* (pp. 1027–1032).
Thienel, J. K., & Sanner, R. M. (2007). Hubble space telescope angular velocity estimation during the robotic servicing mission. *Journal of Guidance, Control, and Dynamics*, *30*(1), 29–34.
Titterton, D. H., & Weston, J. L. (2004). *Strapdown inertial navigation technology* (2nd ed.). The American Institute of Aeronautics and Astronautics.
Trumpf, J., Mahony, R., Hamel, T., & Lageman, C. (2012). Analysis of non-linear attitude observers for time-varying reference measurements. *IEEE Transactions on Automatic Control*, *57*(11), 2789–2800.
Vasconcelos, J. F., Silvestre, C., & Oliveira, P. (2008). A nonlinear observer for rigid body attitude estimation using vector observations. In *Proceedings of the 17th IFAC world congress* (pp. 8599–8604).
Wahba, G. (1965). Problem 65-1: A least squares estimate of spacecraft attitude. *SIAM Review*, *7*(3), 409.

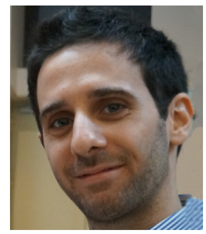

Lionel Magnis was born in 1985 in Saint-Mandé, France. He is teacher of Mathematics at Lyce Claude Bernard, Paris France.

His research interests are in Applied Mathematics with a particular focus on control theory, observer design, and nonlinear filtering.

Dr. Lionel Magnis graduated as Ingénieur civil from MINES ParisTech in 2008, from ENS Cachan in 2012, and obtained his Ph.D. in Mathematics and Control from MINES ParisTech in 2015. Dr. Lionel Magnis holds the Agrégation de Mathématiques.

Nicolas Petit was born in 1972 in Paris, France. He is Professeur at MINES ParisTech and heads the Centre Automatique et Systèmes.

His research interests are in nonlinear control theory. On the application side, he is active in industrial process control, in particular for the petroleum industry and the energy sector. He has founded one startup company and is serving as board member for two others.

Dr. Petit received two times the "Journal of Process Control Paper Prize" for Best article over the periods 2002–2005 and 2008–2011, and is recipient of the 2016 Production and Operations Regional Award from Society of Petroleum Engineers. He has served as an Associate Editor for Automatica over the 2006–2015 period and has been Subject Editor for Journal of Process Control since 2014.

Dr. Petit graduated from Ecole Polytechnique in 1995, and obtained his Ph.D. in Mathematics and Control at Ecole Nationale Supérieure des Mines de Paris in 2000. In 2000–2001, he was a Postdoctoral Scholar in the Control and Dynamical Systems at the California Institute of Technology.